

Protein Science

Stable self-assembly of a protein engineering scaffold on gold surfaces

Samuel Terrettaz, Wolf-Peter Ulrich, Horst Vogel, Qi Hong, Lynn G. Dover and Jeremy H. Lakey

Protein Sci. 2002 11: 1917-1925

Access the most recent version at doi:[10.1110/ps.0206102](https://doi.org/10.1110/ps.0206102)

References

This article cites 37 articles, 8 of which can be accessed free at:
<http://www.proteinscience.org/cgi/content/full/11/8/1917#References>

Article cited in:
<http://www.proteinscience.org/cgi/content/full/11/8/1917#otherarticles>

Email alerting service

Receive free email alerts when new articles cite this article - sign up in the box at the top right corner of the article or [click here](#)

Notes

To subscribe to *Protein Science* go to:
<http://www.proteinscience.org/subscriptions/>

Stable self-assembly of a protein engineering scaffold on gold surfaces

SAMUEL TERRETTAZ,¹ WOLF-PETER ULRICH,¹ HORST VOGEL,¹ QI HONG,² LYNN G. DOVER,² AND JEREMY H. LAKEY^{1,2,3}

¹Institute of Biomolecular Sciences, Swiss Federal Institute of Technology Lausanne, CH-1015 Lausanne, Switzerland

²School of Biochemistry and Genetics, The Medical School, Newcastle upon Tyne, NE2 4HH UK

(RECEIVED February 27, 2002; FINAL REVISION May 15, 2002; ACCEPTED May 16, 2002)

Abstract

The outer membrane protein OmpF from *Escherichia coli* is a member of a large family of β -barrel membrane proteins. Some, like OmpF, are pore-forming proteins while others are active transporters or enzymes. We have previously shown that the receptor-binding domain (R-domain) of the toxin colicin N binds with high affinity to OmpF reconstituted into tethered lipid bilayers on gold electrodes. The binding can be measured by surface plasmon resonance (SPR) and ion channel blockage (impedance spectroscopy, IS). In this paper we report the use of a mutant OmpF-E183C in which a single cysteine had been introduced on a short periplasmic turn. OmpF-E183C binds directly to gold surfaces and creates high-density protein layers by self-assembly from detergent solution. When the gold surface is pretreated with β -mercaptoethanol and thiolipids are added after the protein immobilisation step, the protein is shown, by Fourier transform infrared spectroscopy (FTIR), to retain its β -rich structure. Furthermore, we could also measure R-domain binding by SPR and IS, confirming the functional reconstitution of a self-assembled membrane protein monolayer at the gold surface. Because these β -barrel proteins are recognized protein engineering scaffolds, the method provides a generic method for the simple self-assembly of protein interfaces from aqueous solution.

Keywords: Outer membrane protein; tethered lipid bilayer; FTIR; surface plasmon resonance; impedance spectroscopy; nanotechnology

Protein engineering has made considerable contributions to the understanding of protein structure and function, and with the recent advances of de novo protein design it has opened the door to the creation of new proteins with de-

signed complex properties (Lear et al. 2001; Woolfson 2001). A successful approach in this context is to use structural motifs of existing proteins as stable scaffolds, which, by suitable mutations, deletions, insertions, or fusions create protein structures with desired new functions (Nilsson 1995; Vítá et al. 1995; Skerra 2000). Due to their stable structure, β -sheet and β -barrel proteins figure prominently amongst presently used scaffolds. Bayley et al. have designed molecular sensors for the specific detection of metal ions and organic molecules based on the modulation of the current passing through engineered β -barrel proteins in black lipid membranes (Bayley and Cremer 2001; Gu et al. 1999, 2001). The efficient analysis of the function of channel-forming proteins is an important task in many different fields ranging from (bio)analytics and drug screening to nanoelectronics. Obviously within the rationale of this ap-

Reprint requests to: Jeremy H. Lakey, School of Biochemistry and Genetics, The Medical School, Newcastle upon Tyne, NE2 4HH UK; e-mail: j.h.lakey@ncl.ac.uk; fax: (44)01912227424.

³Visiting professor.

Abbreviations: DOPC: 1,2-dioleoyl-*sn*-glycero-3-phosphocholine; DphyPC: 1,2-diphytanoyl-*sn*-glycero-3-phosphocholine; DP-mercapto-PA: O-(8'-mercapto-3',6'-dioxaoctyl)-1,2-dipalmitoyl-*sn*-glycero-3-phosphatidic acid; DPPC: 1,2-dipalmitoyl-*sn*-glycero-3-phosphocholine; DTT: dithiothreitol; FTIR: Fourier transform infrared spectroscopy; IS: impedance spectroscopy; Omp: outer membrane protein; OPOE: n-Octyl-polyoxyethylene; RA: reflectance absorbance; R-domain: receptor binding domain; SDS: sodium dodecyl sulfate; SPR: surface plasmon resonance.

Article and publication are at <http://www.proteinscience.org/cgi/doi/10.1110/ps.0206102>.

proach, the next step would be the construction of libraries of different molecular sensors where each member would be capable of detecting a different analyte. For efficient analysis devices in a highly parallel format are required, and tethered membranes on multiarray electrodes or planar patch clamping would be realistic possibilities (Heyse et al. 1998; Bieri et al. 1999; Schmidt et al. 2000). Here, we show that β -barrel proteins can be immobilized in an oriented and functionally active form at high density on gold electrodes. This method could be applied to both ion channel analysis and protein array manufacture.

We have chosen to use bacterial outer membrane proteins (Omp) and, in particular, the matrix porin OmpF of *Escherichia coli*, which forms extremely stable 16-stranded β -barrels resistant to proteases, urea, guanidine hydrochloride, sodium dodecyl sulfate (SDS), and heat denaturation (Rosenbusch 1974; Cowan et al. 1992). The high-resolution X-ray-derived structure shows them to be highly asymmetric about the membrane plane with long variable extracellular loops, which are ideal for engineering and short periplasmic turns suitable for interaction with flat gold and semiconductor surfaces. They readily assemble into 2D crystals and have already provided high-quality atomic force microscopy data (Dorset et al. 1983; Schabert et al. 1995; Müller and Engel 1999). They are also gated ion channels that can be closed by voltage and ligands (Schindler and Rosenbusch 1978; Lakey and Pattus 1989; Stora et al. 1999).

In our previous work, we have shown that OmpF in tethered lipid bilayers binds the R-domain of the bacterial toxin Colicin N with a K_d of 0.6–2 μ M. These results were obtained from both surface plasmon resonance (SPR) and resistance changes measured by impedance spectroscopy (IS) (Stora et al. 1999). Recently, it was shown that synthetic ligand gated ion channels, immobilized on gold electrodes can detect antibody binding by conductance changes (Terrettaz et al. 2001).

In the current work we exploit the stability of the porins to create high-density functional arrays of a recombinant Omp scaffold covalently bound to the gold surface. The immobilization to the gold surface is directed by the insertion of a single cysteine residue (E183C) in the fifth periplasmic turn of OmpF. A synthetic thiolipid containing a sulphur-bearing headgroup and a phospholipid are then added sequentially to build a bilayer structure as shown in Figure 1. FTIR spectroscopy is used to probe the conformation of the OmpF protein immobilized on the gold surface and thus find optimal protocols for preserving the native structure of OmpF in the membrane. The amount of protein and lipids adsorbed on the gold surface is monitored by SPR. The function of the resulting proteolipid layer is probed by its ability to bind specific antibodies and the R-domain of Colicin N. While SPR is ideally suited for the surface-sensitive detection of adsorbed molecules, IS measures the channel activity of OmpF.

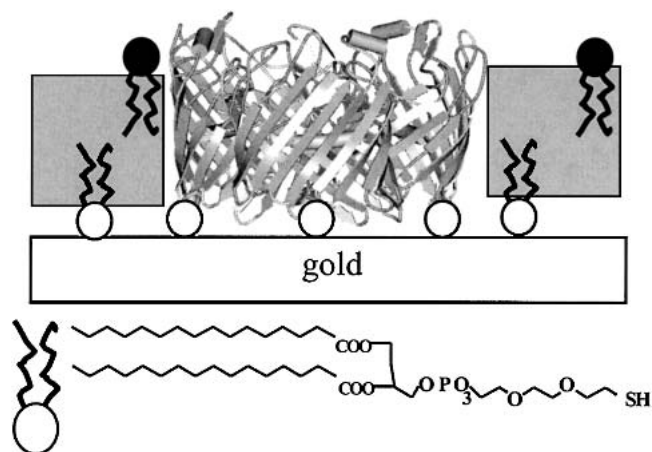


Fig. 1. Schematic illustration of the main features of the chemisorbed proteolipid layer. The structure of the OmpF trimer (Cowan et al. 1992) is shown comprising the E183C cysteine mutations as white ovals. The porin structure was drawn using Weblab (Molecular Simulations Inc.). Each trimer thus has the potential to make three sulphur gold bonds. The thiolipid DP-mercapto-PA (chemical formula shown) is represented by the white oval lipid headgroup, while the mobile lipid DOPC or DPhytPC is shown in black.

Results

Mutant protein production

OmpF-E183C inserted correctly into the outer membrane as judged by its ability to form trimers and its insolubility at low detergent concentrations. It could be solubilized and purified in detergents in the normal way. However, under oxidizing conditions it aggregated and appeared as a ladder of bands on nonreducing SDS-polyacrylamide electrophoresis gels. These aggregates could be disrupted by incubation in 1 mM dithiothreitol (DTT), indicating that the cysteines were exposed and able to form multiple disulphide bridges between porin trimers (data not shown). Self-assembly on gold surfaces was accomplished by samples of freshly reduced (see Materials and Methods) detergent-solubilized trimeric OmpF-E183C. The introduced cysteine prevented removal of the protein from the derivatized gold surface. Wild-type OmpF adsorbed to the derivatized gold electrode but was removed by the subsequent detergent wash (data not shown).

Self-assembly monitored by FTIR

A reference FTIR absorbance spectrum of air-dried multilayers of wild type OmpF is presented in Figure 2A. The amide I band shows the typical shape with a major component at 1630 cm^{-1} and several shoulders between 1650 cm^{-1} and 1670 cm^{-1} and at 1695 cm^{-1} . In agreement with the literature (Nabedryk et al. 1988; Abrecht et al. 2000), the major component at 1630 cm^{-1} and the shoulder at 1695

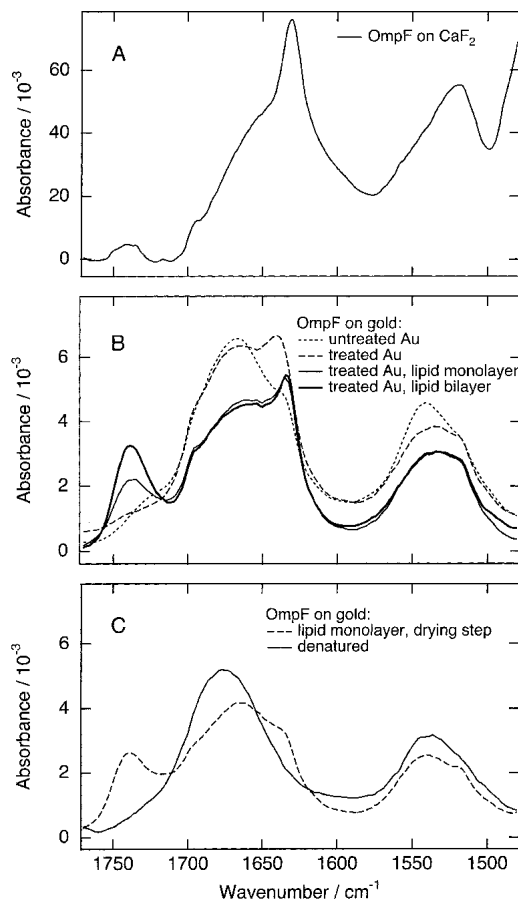


Fig. 2. IR spectra of OmpF layers, showing amide I, II, and the lipid carbonyl band. (A) Bulk OmpF (wild-type) in detergent OPOE on a CaF_2 window in transmission mode. (B and C) RA spectra of OmpF-E183C self-assembled on gold surfaces under various conditions. (B) OmpF-E183C on bare gold (dotted line); OmpF-E183C on mercaptoethanol treated gold (dashed line); mixed layer of OmpF-E183C and DP-mercapto-PA on mercaptoethanol treated gold (thin solid line); mixed layer of OmpF-E183C and DP-mercapto-PA on mercaptoethanol-treated gold including an outer layer of DPhytPC (thick solid line). (C) denatured by boiling in water (solid line), mixed layer of OmpF-E183C and DP-mercapto-PA on mercaptoethanol treated gold with an intermediate drying step (dashed line).

cm^{-1} can be unambiguously assigned to β -sheets. These features are clear indications for the predominance of β -sheet structure in OmpF.

Figure 2B shows IR reflectance absorbance (RA) spectra of OmpF-E183C self-assembled on gold under various conditions. The spectrum of the neat OmpF-E183C layer on bare gold is clearly distinct from the reference spectrum. The maximum is shifted to 1669 cm^{-1} , and only a weak shoulder is discernible at 1639 cm^{-1} . The low β -sheet content of this layer may be attributed to protein unfolding due to a strong interaction of OmpF with the high-energy gold surface. To reduce this unfavorable interaction the gold surface was first treated with β -mercaptoethanol before immo-

bilizing the OmpF. The resulting spectrum of neat OmpF-E183C on such treated gold shows a maximum at 1635 cm^{-1} characteristic for β -sheet contribution but no clear indication for the shoulder at 1695 cm^{-1} . In contrast, the mixed layer of OmpF-E183C and thiolipid O-(8'-mercapto-3',6'-dioxaoctyl)-1,2-dipalmitoyl-*sn*-glycero-3-phosphatidic acid (DP-mercapto-PA) that was prepared under gentle conditions (i.e., without an intermediate drying step) shows an FTIR spectrum with a maximum of amide I at 1633 cm^{-1} and an obvious shoulder at 1695 cm^{-1} . Due to the simplicity of its headgroup, the thiolipid DP-mercapto-PA does not absorb in the amide band region of an FTIR spectrum, which can then be assigned unambiguously to OmpF. The overall intensity of amide I is lower compared to the neat OmpF layer. Typically, about 30% of OmpF is displaced during the self-assembly of DP-mercapto-PA, and this is similar to the amount removed by 1% SDS washes observed by SPR. The peak at $\sim 1740\text{ cm}^{-1}$ is attributed to the carbonyl stretch of the lipid ester bonds. Completion of the bilayer structure was achieved with an outer layer of 1,2-diphytanoyl-*sn*-glycero-3-phosphocholine (DPhyPC) formed by a dilution technique (Terrettaz 1993). The proportional increase in the lipid ester band at $\sim 1740\text{ cm}^{-1}$ is consistent with the formation of an additional lipid monolayer. The maximum of amide I of OmpF-E183C is further downshifted to 1632 cm^{-1} and its intensity is slightly increased.

In an attempt to take an IR spectrum of a highly denatured OmpF, a preformed OmpF layer on gold was boiled in water for 10 sec. The resulting spectrum is shown in Figure 2C. The maximum of the amide I contour is shifted to higher wavenumbers (1677 cm^{-1}) compared to the untreated neat OmpF layer on gold. Only a weak shoulder appears at 1642 cm^{-1} . These are clear indications for the virtual absence of any β -sheet in this sample. Figure 2C also shows another spectrum of a mixed layer of OmpF and DP-mercapto-PA on β -mercaptoethanol-treated gold. In this case, the sample has been air dried prior to the addition of DP-mercapto-PA. The respective spectrum of the OmpF layer before the thiolipid was added is shown in Figure 2B. Upon addition of thiolipid the intensity of the peak at 1635 cm^{-1} decreases strongly. This peak intensity is then much smaller than in the corresponding spectrum of a mixed layer obtained in the absence of any air-drying step between OmpF and thiolipid addition (Fig. 2B, thin solid line).

With increasing complexity of the layer structure the low wave number component of amide I located at $1630\text{--}1640\text{ cm}^{-1}$ evolves from a minor contribution at 1639 cm^{-1} to a major contribution at 1632 cm^{-1} . This clearly indicates an increase in the β -sheet content and in the length of the β -strands (Goormaghtigh et al. 1994). It underlines the importance of: (1) avoiding any drying step during the multistep procedure that leads to the formation of the mixed layer, and (2) blocking the highly energetic gold surface with an agent like β -mercaptoethanol or the previously used

sulfanylpropionic acid (Stora et al. 1999). A qualitative comparison of amide I of OmpF-E183C incorporated in the DP-mercapto-PA /DPhyPC layer (Fig. 2B, thick solid line) with native OmpF (Fig. 2A) reveals a somewhat lower β -sheet content in the tethered layer. From our results, it is reasonable to assume that this is largely caused by a combination of the interaction of OmpF with the surface and the drying event prior to FTIR spectroscopy.

Apart from conformational information considered so far, it would be instructive to derive orientational information from the IR data. RA measurements on metal surfaces have been proven capable of probing protein orientation (Boncheva and Vogel 1997). The surface selection rule (Greenler 1996) states that only parallel-polarized light with respect to the plane of incidence can be absorbed from thin layers on metal surfaces. Thus, the dichroic ratio of parallel and perpendicular polarization generally used to determine helix orientation on ATR plates (Thiaudière et al. 1993; Tamm and Tatulian 1997) is not accessible in RA spectroscopy. Instead, one favorably exploits the ratio of intensities of amide I/II bands. However, in the given case the orientation of the barrel with respect to the surface normal cannot be determined. It has been shown (Tamm and Tatulian 1997; Marsh 2000) that the amide I and II modes are distributed with axial symmetry about the barrel axis and exhibit virtually the same angle of about 45° with respect to the barrel axis. Consequently, the amide I/II band intensity ratio depends only weakly on the barrel orientation.

Self-assembly monitored by SPR

The conditions for an optimal adsorption of OmpF-E183C on gold surfaces as worked out by FTIR measurements have been used for preparing layers with a high-density of OmpF at gold surfaces. In the case of a sequential addition of layers, SPR allows a direct measurement of the amount of OmpF-E183C chemisorbed from a detergent solution. (Fig. 3). The shift of the resonance angle of $(0.31^\circ \pm 0.07^\circ, n = 5)$ obtained at steady state was largely independent of the exact composition of the solution as long as the porin concentration was superior to 6×10^{-7} M. Making use of the refractive index increment for proteins, $dn/dc = 0.18 \text{ g}^{-1}\text{cm}^3$, a mean molecular area of $13200 \text{ \AA}^2/\text{molecule}$ is calculated from this angular shift independently on the actual value of the refractive index. Considering the molecular dimensions of a trimer as an equilateral triangle with sides 80 \AA long, the obtained coverage corresponds then to 21% of a full monolayer of OmpF and one half of the density of reported two-dimensional crystals whose packing consisted of two trimer molecules per unit rectangular cell of $135 \times 82 \text{ \AA}^2$ (Schabert et al. 1995). The average thickness of a monolayer can be derived from the experimentally obtained angle shift if the actual value of the refractive index is known. For proteins, the refractive index is usually between 1.45 and

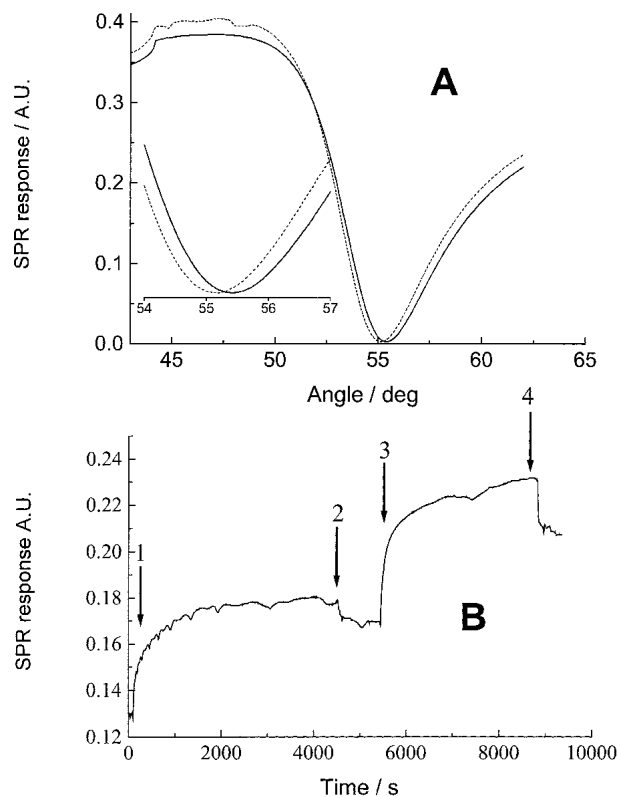


Fig. 3. (A) SPR resonance curve before and after adsorption of OmpF-E183C on a gold surface coated with a self-assembled monolayer of mercaptoethanol. The shift of resonance angle of 0.31° characterizes the amount of protein adsorbed, which corresponds to an apparent monolayer with a mean molecular area of 13200 \AA^2 . (B) Sequential adsorption of OmpF-E183C and DP-mercapto-PA measured as an increase of the intensity of the reflected beam at an angle of ca. 1° lower than the resonance angle. Arrows show (1) replacement of protein-free 1% OPOE solution by equivalent solution containing 0.3 mg/mL OmpF-E183C, (2) wash with protein-free 1% OPOE solution, (3) replacement by solution containing 1 mg/mL DP-mercapto-PA in 1% OPOE solution, (4) wash with 1% OPOE solution.

1.5. An angular shift of 0.31° corresponds to a monolayer of 19.8 and 14 \AA , assuming a refractive index of 1.45 and 1.50 , respectively. The latter thickness is in good agreement with the value expected for a monolayer of the density calculated above because the porin is approximately 50 \AA high (Cowan et al. 1992) and porin-lipid monolayers on mica have been reported to be 61 \AA thick by atomic force microscopy. (Schabert et al. 1995).

The increase of mass obtained after the successive adsorption of the DP-mercapto-PA and DphyPC corresponds to the values reported for full monolayers of the thio- and the phospholipids, respectively (Lang et al. 1994). Considering the space occupied by the porin, SPR experiments show that slightly more than a single monolayer of DP-mercapto-PA and DPhyPC are sequentially added to these OmpF-coated gold electrodes.

The beneficial role of a short-chain ω -hydroxythioalkane layer should be highlighted. In addition to its protective function revealed by FTIR, this short layer did not diminish the access of OmpF to the gold surface. Indeed, the values obtained at saturation were very similar in the presence and in the absence of a mercaptoethanol monolayer. The insertion of OmpF-E183C can occur either through defects in the ω -hydroxythioalkane layer or through a replacement of a small number of thiols similarly to a process described earlier (Bain et al. 1989). This very simple protocol allows a better control of the OmpF density at the gold surface than any coadsorption with short hydrophilic spacers. It also represents a very convenient way to store gold surfaces in mercaptoethanol solutions before any subsequent adsorption step. Three-day aging in a 50 mM solution of mercaptoethanol proved to have no measurable influence on the OmpF adsorption that followed, and we expect this to be true over a much longer period of time.

Function of layers monitored by SPR

OmpF/DP-mercapto-PA/DOPC (1,2-dioleoyl-*sn*-glycero-3-phosphocholine) layers were used in the Biacore system to measure protein-protein interactions between the OmpF-E183C and ligands. A rabbit polyclonal antiloop 6 antibody (Bainbridge et al. 1998) bound to the porin with high affinity ($K_d = 1.4$ nM, results not shown) but, although this provides evidence for the correct orientation of the porin, it is not evidence for conformational integrity. For this we used the R-domain of colicin N, which has been shown to bind to the outer surface of OmpF with affinities in the range $K_d = 0.6$ – 2 μ M (Evans et al. 1996b; Stora et al. 1999). The high sensitivity of the Biacore apparatus was exploited to measure protein adsorption at very low concentrations of the R-domain. A range of R-domain concentrations between 40 and 320 nM were injected over OmpF thiolipid layers. Analysis of the sensorgrams for a range of R-domain concentrations (Fig. 4) indicated that the data were consistent with a 1:1 interaction (Evans et al. 1996a) with a K_d of 0.1 μ M (± 0.01 , $n = 2$).

Function of layers monitored by impedance spectroscopy

Proteolipid layers with a high-density of OmpF-E183C have impedance spectra that are dominated by the electrode/electrolyte interface at all frequencies. The impedance parameters describing the proteolipid layers are only obtained for layers with a higher resistance. In the present case, such layers were produced by increasing the lipid-to-protein ratio. The impedance spectra could then be fitted by the simple equivalent circuit shown in the insert of Figure 5A. The low-frequency part of the impedance spectra (1 to 100 Hz) was dominated by the double-layer capacitance, C_{dl} . Its

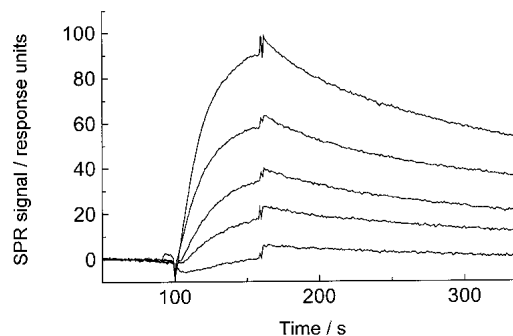


Fig. 4. An OmpF/ DP-mercapto-PA/DOPC layer of approximately 800 RU OmpF was formed as a sequential assembly. The R-domain solution was added in 0.3 M NaCl, 0.1 M KCl, 0.1 M potassium phosphate buffer. The sensorgrams show injections of 40, 80, 120, 200, and 320 nM solutions of R-domain as a difference signal between the OmpF and non OmpF containing lipid bilayers. Fits to these data using a standard single-site model gave a K_d of 100 nM. Flow rate was 5 μ L min^{-1} .

value was seen to be practically identical to the capacitance of the protective ω -hydroxythioalkane layer. A capacitance value of 0.6 ± 0.1 $\mu\text{F}/\text{cm}^2$ was obtained for the lipid bilayer from the high-frequency range of the impedance spectra. This measured capacitance was similar to values reported for “suspended”, that is, unsupported, black lipid membranes indicating a lipid bilayer with a high degree of integrity. The resistance of the supported lipid bilayer was considerably lower than for suspended lipid bilayers as often reported (Steinem et al. 1997; Gritsch et al. 1998; Stora et al. 1999; Terrettaz et al. 2001). A modulation of the layer resistance by ligand binding has been shown in a few cases (Cornell et al. 1997; Gritsch et al. 1998; Stora et al. 1998; Terrettaz et al. 2001). The value of our layer resistance depended on the lipid-to-protein ratio, and varied between 10^3 to 10^5 Ω . The increase of the layer resistance by R-domain binding could be directly followed as the increase of the real part of the impedance Z_r , in the plateau range between 10 to 200 Hz (Fig. 5B). The major part of the response could be reversed by washing with buffer because the fraction of rebound R-domain was very small at this low density of surface-bound OmpF. Very little response was obtained at submicromolar concentrations of R-domain. An approximately 10% increase of the resistance could be obtained at larger R-domain concentrations. These results are in good quantitative agreement with data obtained with the wild type OmpF reconstituted in a lipid bilayer (Stora et al. 1999). Currently, the number of defects in the supported lipid layers limits the sensitivity of the detection. Gating of a single channel protein can be detected by electrical techniques if the layer resistance is in the gigaohm range as in patch-clamp systems. The supported lipid layers presented here displayed, however, a remarkable stability unparalleled by suspended lipid bilayers.

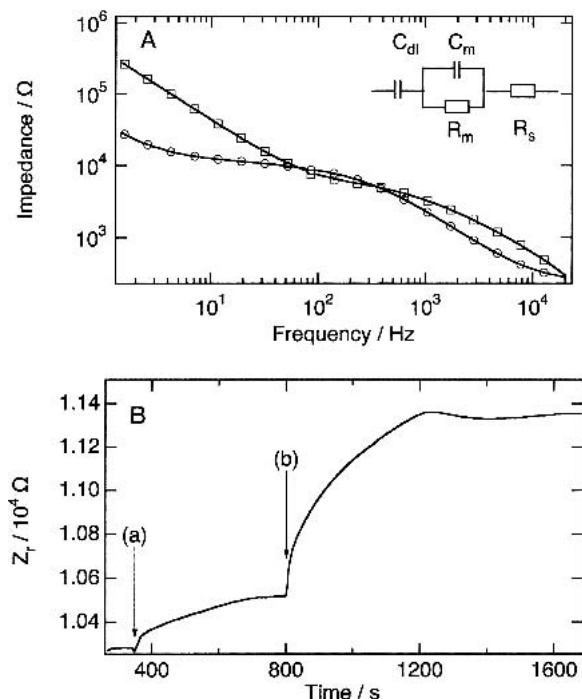


Fig. 5. (A) Real (open circles) and imaginary (open squares) parts of the electrical impedance spectrum of a 3.34-mm² disk gold electrode covered with an OmpF-containing lipid bilayer. A monolayer of mercaptobutanol was first self-assembled on the electrode prior to the adsorption of OmpF-E183C. The lipid bilayer was then completed by overnight incubation with DP-mercapto-PA in an octyl glucoside solution followed by a slow dilution with buffer. Only each tenth measured point is shown. The data were interpreted through the electrical circuit depicted in the insert. The proteolipid bilayer is described by a parallel combination of the resistance R_m and the capacitance C_m , while C_{dl} and R_s represent the double-layer capacitance and the solution resistance, respectively. (B) Real part of the electrical impedance (measured at 30 Hz) of a lipid bilayer containing the porin OmpF-E183C after the addition of 2 μ M (a) and 10 μ M (b) of the receptor binding domain of Colicin N.

Discussion

The results show that high densities of functional OmpF can be easily self-assembled from aqueous solution to create a proteolipid layer at a plane gold surface. The denaturing action of the bare gold is striking and, although reported previously, its effects on these otherwise robust proteins confirm the need for methods to mitigate these effects. The surface is considered hydrophobic, but the extent of denaturation observed requires further explanation. The denaturation of the protein is clearly exacerbated by the drying step required for FTIR measurements because an intermediate drying step before thiolipid addition results in a significant increase in denaturation. As a result, the precise extent of denaturation of OmpF in the full proteolipid layer is unclear. The comparison with published spectra indicates a significant retention of β -structure but whether the remaining loss occurs during the drying step is currently impossible to

determine. The insertion of the cysteine into the tight turn at the edge of the trimer may also contribute to the forces acting on the immobilized protein because the base of the protein is not planar and three covalent bonds per trimer may impose tension on the structure. Nevertheless, the data shows that a combination of surface treatment with short hydrophilic thiols and stabilization with thiolipids provides the basis for the straightforward reconstitution of membrane proteins at this inhospitable interface. In particular, the reproducibility of the layer density shows that this is a protein-directed self-assembly step that is concentration- and reagent-independent.

The lack of an enzymatic activity means that assaying porin function at the interface relies upon its pore formation and ligand binding activity. The effect of R-domain binding on the pore activity has already been well characterized in tethered lipid bilayers and the results from the directly immobilized protein fit to the previous model. First, the layer with immobilized porin contributes a distinct RC component visible in the 100-Hz region, and second, the resistive component of the impedance increases when R-domain is added. As with the earlier study, the density of porins needs to be very low to prevent saturation of the conductance.

Although antibody binding to exposed loops of OmpF is measurable by SPR, these epitopes are not conformation-sensitive, and denatured proteins are recognized as well. The interface with the colicin R-domain is a better test because it is dependent upon the conformation of OmpF, requires the correct orientation, correlates with the known IS data (Stora et al. 1999) and is of lower affinity. The binding observed in the Biacore showed low nonspecific binding because binding of R-domain to the reference channel composed of lipids only was negligible. The binding affinity was slightly higher than in the previous study on tethered lipid layers (0.1 μ M compared to 0.6 μ M).

The techniques used here should be applicable to other outer membrane proteins (of which there are 500 examples in the Swissprot Database) which include transporters, enzymes, and cell adhesion proteins. Their use may allow precise study of their functions and perhaps allow for screening of clinical samples from pathogenic Gram-negative bacteria such as *Neisseria* (Mee et al. 1993). However, it may be in the possibilities of Omp as cell surface display and protein engineering scaffolds that the most widespread use of this technique may be achieved (Lang 2000). Rapid assembly of such a range of surfaces with both optical and electrical readout is likely to have many applications. In particular, electrical biosensors of utmost sensitivity can be envisioned if the intrinsic amplification provided by ion-channel ligand gating is fully exploited. This will modulate the flux of millions of ions per second as the result of a single molecular interaction. The self-assembly of high-density supported proteolipid layers is an important step toward this goal.

Materials and methods

Chemicals

1,2-Diphytanoyl-*sn*-glycero-3-phosphocholine (DPhyPC) and 1,2-dioleoyl-*sn*-glycero-3-phosphocholine (DOPC) were from Avanti Polar Lipids (Alabaster). *n*-Octyl-polyoxyethylene with 1 to 10 oxyethylene units (OPOE) was from Alexis, octylglucoside from Bachem, and dithiothreitol (DTT) was from Sigma. Other chemicals were from Fluka, and were of the highest purity available. The water used was purified via an exchanger purification train (Milli-Q system, Millipore).

Production of OmpF mutant proteins

OmpF-E183C was prepared by Quickchange (Stratagene Inc.) site-directed mutagenesis, and purified as described previously (Bainbridge et al. 1998). All samples showed affinity for gold, but the most consistent results were obtained with protein that had been reduced in 1 mM DTT at 37°C for 1 h. DTT was removed by using a PD-10 (Pharmacia) column preequilibrated with buffer containing 1% detergent. 0.5 mL of reduced protein was applied to the column and chased with 2 mL of buffer. The protein eluted in the following 1 mL and the sample was used that day.

Synthesis of thiolipid DP-mercapto-PA

The thiolipid O-(8'-mercapto-3',6'-dioxaoctyl)-1,2-dipalmitoyl-*sn*-glycero-3-phosphatidic acid (DP-mercapto-PA; Fig. 1) was synthesized from 1,2-dipalmitoyl-*sn*-glycero-3-phosphocholine (DPPC; Fluka) via a phosphoester exchange reaction of the choline group by 1-mercaptotriethyleneglycol in the presence of phospholipase D (Sigma). To our knowledge, this was the first time that a thiolipid was synthesized according to this procedure, and we wish to emphasize the simplicity of synthesis. Two hundred micromoles of 1-mercapto-triethyleneglycol were dissolved together with 50 units of phospholipase D in 0.1 mL reaction buffer (100 mM sodium acetate, 50 mM CaCl₂, pH 6.5). A solution of 40 μmol DPPC in 0.8 mL ethanol-free chloroform was added, and the dispersion was shaken at 35°C for 4 h. The organic phase was separated after centrifugation, washed three times with buffer (10 mM Na-EDTA, 10 mM sodium phosphate pH 7.4), and purified by column chromatography.

¹H-NMR (CDCl₃:CD₃OD 4:1, 200 MHz): δ 5.22 (m, 1H, H—C(2)); 4.38, 4.17 (2dd, *J* = 12, 3.5, and *J* = 12, 6.5, 2H, H—C(1)); 4.00 (m, 4H, CH₂OPOCH₂); 3.7–3.6 (br.s, 8H, H—C(4',5',7',8')); 2.69 (t, *J* = 6.5, 2H, —S—CH₂); 2.31 (dt, *J* = 7.5, 2.5, 4H, CH₂CH₂CO); 1.59 (m, 4H, CH₂CH₂CO); 1.26 (br.s, 32H, CH₂-fatty acids); 0.88 (t, *J* = 6.5, 6H, CH₃-fatty acids).

³¹P-NMR (CDCl₃:CD₃OD 4:1, 100 MHz): δ -43.2.

MS (ESI); 797.4 (M⁺ without Na⁺).

C₄₁H₈₀O₁₀PSNa (M = 819.1).

Preparation of supported self-assembled layers

Glass slides were cleaned by ultrasonication first in the detergent solution "Hellmanex" (Hellma) and then in pure water. For surface plasmon measurements, SF10 glass slides (Ginchar S.A.) with an index of refraction *n* = 1.723 were used. Gold layers of 45-nm thickness were evaporated on glass samples at a pressure of 5 × 10⁻⁶ bar. For FTIR measurements, gold layers of more than

100 nm were prepared to avoid back reflection from the glass support. The adhesion of the gold layer to the glass surface was improved by deposition of an intermediate 1-nm thick chromium (Balzers) layer or by silanization of the glass surface with 3-mercaptopropyltrimethoxy-silane (Aldrich). The latter procedure was mainly used for impedance measurements. After being cooled to room temperature in the vacuum chamber, the gold-coated glass slides were transferred immediately to ω-hydroxythioalkane or buffer solutions and subsequently mounted in the different measuring cells.

To avoid protein denaturation, gold electrodes were generally first coated by a monolayer of ω-hydroxythioalkane (HO—(CH₂)*n*-SH, with *n* = 2, 4, and 6) self-assembled from an ethanolic solution. OmpF-E183C was adsorbed from a 1% detergent solution (SDS or OPOE) containing concentrations superior to 6 × 10⁻⁷ M for FTIR and SPR. The same limiting OmpF coverage was obtained at saturation within this concentration range. Porin concentrations of less than 6 × 10⁻⁹ M were used to get the high thiolipid-to-protein ratio necessary for a high membrane impedance. The surface-immobilized OmpF was first integrated into a tethered lipid monolayer by adding DP-mercapto-PA from an octyl glucoside solution. The lipid bilayer was then completed by an additional monolayer of DPhyPC or DOPC formed by dilution below the critical micellar concentration of the detergent used (Terrettaz et al. 1993). Binding of the R-domain protein to the sensor surface at constant protein concentration in the bulk was measured as described earlier (Stora et al. 1999).

FTIR measurements

Infrared spectra were recorded using a Bruker IFS 28 spectrometer equipped with an HgCdTe detector. One thousand scans were recorded at 1 cm⁻¹ resolution and apodized with a boxcar function. Background spectra were recorded from the respective bare supports. For the precise subtraction of spectral contributions from water vapor, we employed the procedure described by (Goormaghtigh et al. 1994). The corrected spectra were Fourier smoothed to 4 cm⁻¹ resolution with triangular apodization. Absorbance spectra of wild-type OmpF as bulk solid samples were obtained in transmission mode by air drying solutions of OmpF in 1% OPOE on precleaned CaF₂ windows. RA spectra of molecular layers on gold were recorded at an angle of incidence of 85° of parallel-polarized light. All peak positions were derived from second derivative spectra (Goormaghtigh et al. 1994).

Surface plasmon resonance (SPR)

SPR measurements were performed on a home-made reflection apparatus (Terrettaz et al. 1993) and a Biacore-X (Biacore AB). Assuming a refractive index of *n* = 1.45, an experimental shift of 1° or 10,000 resonance units (RU) corresponded to a layer thickness of 6.4 nm for the home-made and 7.6 nm for the Biacore instrument. The angle shift obtained at steady state was used to characterize the molecular layers, while the kinetics of layer formation was monitored at an angle slightly lower than the resonance angle at the steepest part of the resonance curve. For thin adsorbed layers (<50 nm) the measured angle shift Δθ was proportional to the product (*d* Δ*n*), where *d* is the geometrical thickness of the layer and Δ*n* is the difference between the real refractive indices of the layer and the medium. The layer thickness was further calculated by assuming a refractive index of 1.45 and 1.5 for lipid and proteins, respectively (Terrettaz et al. 1993). The mean molecular area of adsorbed proteins in a layer was calculated

independently on the actual value of the refractive index as $A = (m \, dn/dc)/(d \, \Delta n)$, where m is the mass of the corresponding protein molecule, $dn/dc = 0.18 \, \text{cm}^3 \text{g}^{-1}$ is the refractive index increment, and $(d \, \Delta n)$ was directly derived from the measured angle shift. In the Biacore proteolipid layers were formed using sequential assembly on mercaptoethanol treated plain gold J1 chips (Biacore) using a Biacore-X apparatus. OmpF-E183C (0.3 mg/mL) in OPOE solution at a flow rate of $5 \, \mu\text{L min}^{-1}$ was used to form the protein layer. This was washed with 1% SDS to remove noncovalently bound OmpF, DP-mercapto-PA dissolved in 1% OPOE was then added, followed by DOPC vesicles (1 mg/mL) to complete the layer. The reference channel was identical except for the OmpF treatment. Binding experiments were run at 25°C and at a higher flow rate of $30 \, \mu\text{L min}^{-1}$ to minimize mass transport effects. As with previous experiments with colicin N, 300 mM NaCl was added to the running buffer to prevent colicin aggregation thus phosphate buffer (0.1 M potassium phosphate, 0.1 M KCl, 0.3 M NaCl pH 7.4) filtered through a $0.22 \, \mu\text{m}$ Millipore filter and degassed in vacuum was used as the running buffer in all experiments. Every binding experiment performed included a reference surface containing a protein free DOPC/ DP-mercapto-PA bilayer. The binding kinetics of the interaction between the functional porin layer and the analyte (R-domain or antibody) were then measured by passing a concentration series over the sensor chip. Affinity parameters were determined by fitting kinetic sensorgrams to a Langmuir adsorption isotherm model as described previously (Gokce et al. 2000).

Impedance spectroscopy (IS)

IS was done in an electrochemical cell comprising a membrane-covered gold electrode and a counter/reference Ag/AgCl electrode in 0.5 M KCl/5 mM sodium phosphate buffer, pH 7.4. The surface area of the gold disk electrode was $3.34 \times 10^{-2} \, \text{cm}^2$. No DC voltage was applied. A sinusoidal voltage of 10 mV amplitude (root-mean-square) was applied to the cell at 199 successive frequencies equally spaced on a logarithmic scale from 1 Hz to 20 KHz. The resulting current was recorded via a phase-sensitive lock-in amplifier to calculate the complex impedance and admittance. The value of the different equivalent circuit elements was obtained from a complex nonlinear least squares fit of the impedance spectra (MacDonald 1987).

Acknowledgments

J.H.L. thanks the UK Biotechnology and Biological Sciences Research Council for the continued financial support, which has enabled this project to develop; the Wellcome Trust for equipment grant 056232; and the Ecole Polytechnique Fédérale de Lausanne for a Visiting Professorship. H.V. thanks the EPFL for continuous financial support. We thank Pauline Heslop for excellent technical assistance, Andreas Heusler and Dr. Zoltan Dienes for synthesis of thiolipids, and Dr. Claus Duschl for lively discussions and sound advice.

The publication costs of this article were defrayed in part by payment of page charges. This article must therefore be hereby marked "advertisement" in accordance with 18 USC section 1734 solely to indicate this fact.

References

Abrecht, H., Goormaghtigh, E., Ruysschaert, J.M., and Homble, F. 2000. Structure and orientation of two voltage-dependent anion-selective channel iso-

- forms. An attenuated total reflection Fourier-transform infrared spectroscopy study. *J. Biol. Chem.* **275**: 40992–40999.
- Bain, C.D., Troughton, E.B., Tao, Y.-T., Evall, J., Whitesides, G.M., and Nuzzo, R.G. 1989. Formation of monolayer films by the spontaneous assembly of organic thiols from solution onto gold. *J. Am. Chem. Soc.* **111**: 321–335.
- Bainbridge, G., Mobasheri, H., Armstrong, G.A., Lea, E.J.A., and Lakey, J.H. 1998. Voltage gating of *Escherichia coli* porin; A cysteine scanning mutagenesis study of loop 3. *J. Mol. Biol.* **275**: 171–176.
- Bayley, H. and Cremer, P.S. 2001. Stochastic sensors inspired by biology. *Nature* **413**: 226–230.
- Bieri, C., Ernst, O.P., Heyse, S., Hofmann, K.P., and Vogel, H. 1999. Micro-patterned immobilization of a G protein-coupled receptor and direct detection of G protein activation. *Nat. Biotechnol.* **17**: 1105–1108.
- Boncheva, M. and Vogel, H. 1997. Formation of stable polypeptide monolayers at interfaces: Controlling molecular conformation and orientation. *Biophys. J.* **73**: 1056–1072.
- Cornell, B.A., Braach-Maksyvtis, V.L.B., King, L.G., Osman, P.D.J., Raguse, B., Wiczorek, L., and Pace, R.J. 1997. A biosensor that uses ion-channel switches. *Nature* **387**: 580–583.
- Cowan, S.W., Schirmer, T., Rummel, G., Steiert, M., Ghosh, R., Paupit, R.A., Jansonius, J.N., and Rosenbusch, J.P. 1992. Crystal structures explain functional properties of two *E. coli* porins. *Nature* **358**: 727–733.
- Dorset, D.L., Engel, A., Haner, M., Massalski, A., and Rosenbusch, J.P. 1983. Two-dimensional crystal packing of matrix porin—A channel forming protein in *Escherichia coli* outer membranes. *J. Mol. Biol.* **165**: 701–710.
- Evans, L.J.A., Cooper, A., and Lakey, J.H. 1996a. Direct measurement of the association of a protein with a family of membrane receptors. *J. Mol. Biol.* **255**: 559–563.
- Evans, L.J.A., Labeit, S., Cooper, A., Bond, L.H., and Lakey, J.H. 1996b. The central domain of colicin N possesses the receptor recognition site but not the binding affinity of the whole toxin. *Biochemistry* **35**: 15143–15148.
- Gokce, I., Raggett, E.M., Hong, Q., Virden, R., Cooper, A., and Lakey, J.H. 2000. The TolA-recognition site of colicin N. ITC, SPR and stopped-flow fluorescence define a crucial 27-residue segment. *J. Mol. Biol.* **304**: 621–632.
- Goormaghtigh, E., Cabiaux, V., and Ruysschaert, J.-M. 1994. Determination of soluble and membrane protein structure by Fourier transform infrared spectroscopy. I. Assignments and model compounds. In *Physicochemical methods in the study of biomembranes* (eds. H.J.Hilderson and G.B. Ralston), vol. 23, pp. 329–361. Plenum, New York.
- Greenler, R.G. 1966. Infrared study of adsorbed molecules on metal surfaces by reflection techniques. *J. Chem. Phys.* **44**: 310–315.
- Gritsch, S., Nollert, P., Jahnig, F., and Sackmann, E. 1998. Impedance spectroscopy of porin and gramicidin pores reconstituted into supported lipid bilayers on indium-tin-oxide electrodes. *Langmuir* **14**: 3118–3125.
- Gu, L., Braha, O., Conlan, S., Cheley, S., and Bayley, H. 1999. Stochastic sensing of organic analytes by a pore-forming protein containing a molecular adapter. *Nature* **398**: 686–690.
- Gu, L.Q., Cheley, S., and Bayley, H. 2001. Capture of a single molecule in a nanocavity. *Science* **291**: 636–640.
- Heyse, S., Stora, T., Schmid, E., Lakey, J.H., and Vogel, H. 1998. Emerging techniques for investigating molecular interactions at lipid membranes. *Biochim. Biophys. Acta* **1376**: 319–338.
- Lakey, J.H. and Pattus, F. 1989. The voltage-dependent activity of *Escherichia coli* porins in different planar bilayer reconstitutions. *Eur. J. Biochem.* **186**: 303–308.
- Lang, H. 2000. Outer membrane proteins as surface display systems. *Int. J. Med. Microbiol.* **290**: 579–585.
- Lang, H., Duschl, C., and Vogel, H. 1994. A new class of thiolipids for the attachment of lipid bilayers on gold surfaces. *Langmuir* **10**: 197–210.
- Lear, J.D., Gratkowski, H., and DeGrado, W.F. 2001. De novo design, synthesis and characterization of membrane-active peptides. *Biochem. Soc. Transact.* **29**: 559–564.
- MacDonald, J.R. 1987. *Impedance spectroscopy*. John Wiley and Sons Inc., New York.
- Marsh, D. 2000. Infrared dichroism of twisted beta-sheet barrels. The structure of *E-coli* outer membrane proteins. *J. Mol. Biol.* **297**: 803–808.
- Mee, B.J., Thomas, H., Cooke, S.J., Lambden, P.R., and Heckels, J.E. 1993. Structural comparison and epitope analysis of outer-membrane protein Pla from strains of *Neisseria gonorrhoeae* with differing serovar specificities. *J. Gen. Microbiol.* **139**: 2613–2620.
- Müller, D.J. and Engel, A. 1999. Voltage and pH-induced channel closure of porin OmpF visualized by atomic force microscopy. *J. Mol. Biol.* **285**: 1347–1351.
- Nabedryk, E., Garavito, R.M., and Breton, J. 1988. The orientation of beta-

- sheets in porin—A polarised Fourier-transform infrared spectroscopic investigation. *Biophys. J.* **53**: 671–676.
- Nilsson, B. 1995. Antibody engineering. *Curr. Opin. Struct. Biol.* **5**: 450–456.
- Rosenbusch, J.P. 1974. Characterisation of the major envelope protein from *Escherichia coli*. *J. Biol. Chem.* **249**: 8019–8029.
- Schabert, F.A., Henn, C., and Engel, A. 1995. Native *Escherichia coli* OmpF porin surfaces probed by atomic-force microscopy. *Science* **268**: 92–94.
- Schindler, H. and Rosenbusch, J.P. 1978. Matrix protein from *Escherichia coli* outer membranes forms voltage controlled channels in lipid bilayers. *Proc. Natl. Acad. Sci.* **75**: 3751–3755.
- Schmidt, C., Mayer, M., and Vogel, H. 2000. A chip-based biosensor for the functional analysis of single ion channels. *Angew. Chem. Int. Ed.* **39**: 3137–3140.
- Skerra, A. 2000. Engineered protein scaffolds for molecular recognition. *J. Mol. Recognit.* **13**: 167–187.
- Steinem, C., Janshoff, A., Galla, H.J., and Sieber, M. 1997. Impedance analysis of ion transport through gramicidin channels incorporated in solid supported lipid bilayers. *Bioelectrochem. Bioenerget.* **42**: 213–220.
- Stora, T., Lakey, J.H., and Vogel, H. 1999. Ion-channel gating in transmembrane receptor proteins: Functional activity in tethered lipid membranes. *Angew. Chem. Int. Ed.* **38**: 389–392.
- Tamm, L.K. and Tatulian, S. 1997. Infrared spectroscopy of proteins and peptides in lipid bilayers. *Q. Rev. Biophys.* **30**: 365–429.
- Terrettaz, S., Stora, T., Duschl, C., and Vogel, H. 1993. Protein binding to supported lipid membranes; Investigation of the Cholera Toxin–Ganglioside interaction by simultaneous impedance spectroscopy and surface plasmon resonance. *Langmuir* **9**: 1361–1369.
- Terrettaz, S., Ulrich, W.P., Guerrini, R., Verdini, A., and Vogel, H. 2001. Immunosensing by a synthetic ligand-gated ion channel. *Angew. Chem. Int. Ed.* **40**: 1740–1743.
- Thiaudière, E., Soekarjo, M., Kuchinka, E., Kuhn, A., and Vogel, H. 1993. Structural characterization of membrane insertion of M13 and Pf3 coat proteins. *Biochemistry* **32**: 12186–12196.
- Vita, C., Roumestand, C., Toma, F., and Menez, A. 1995. Scorpion toxins as natural scaffolds for protein engineering. *Proc. Natl. Acad. Sci.* **92**: 6404–6408.
- Woolfson, D.N. 2001. Core-directed protein design. *Curr. Opin. Struct. Biol.* **11**: 464–471.